sciendo

Int. J. Appl. Math. Comput. Sci., 2025, Vol. 35, No. 3, 443–454
DOI: 10.61822/amcs-2025-0031

amcs

AN ITERATIVE LEARNING CONTROL APPROACH TO SENSOR FAULT–TOLERANCE IN TAKAGI–SUGENO SYSTEMS

MARCIN PAZERA [a], BARTŁOMIEJ SULIKOWSKI [a,*], MARCIN WITCZAK [a]

[a]Institute of Control and Computation Engineering
University of Zielona Góra
ul. prof. Z. Szafrana 2, 65-516 Zielona Góra, Poland
e-mail: {m.pazera,b.sulikowski,m.witczak}@issi.uz.zgora.pl

This paper presents a solution to the problem of effective control of a system that is affected by both sensor faults and disturbances (and noises). It is assumed that the model of the system is given in the form of a fuzzy Takagi–Sugeno system. The main goals of the designed control scheme are: achieving a prescribed reference signal at the output, minimizing the impact of disturbances and the ability to respond to faults affecting the system sensor. To achieve the assumed control goals an Iterative Learning Control (ILC) scheme combined with the Fault Tolerant Control (FTC) approach is implemented. Such a combination allows detecting and using information of the faults affecting the system as soon as these are estimated. That in turns speeds up ILC with driving the system to the prescribed reference. Additionally, to determine the estimate of the fault signal and the faulty-free state vector, the observer providing these is designed and implemented. To minimize the impact of disturbances on the estimator, the $\mathcal{H}_\infty$ methodology is used. The determined estimate of the fault-free state signal is then introduced into the ILC scheme in order to improve its operation in the presence of fault. To determine gains in the feedback loop of the ILC scheme, it is formulated in the form of a Discrete Linear Repetitive Process (DLRP), and then a methodology designed for that subclass of 2D systems is applied to ensure the so-called stability along the trial (which simultaneously means that the underlying ILC scheme tracking error converges to zero and, consequently, the system considered is driven to the requested reference signal). In order to minimize the impact of disturbances and noises on the designed ILC scheme, the $\mathcal{H}_\infty$ methodology is used again. The obtained results are verified practically in the control process of the two-tank system with the assumed scenarios of emerging faults.

Keywords: fault-tolerant control, iterative learning control, sensor faults, Takagi–Sugeno systems.

1. Introduction

Over the years Iterative Learning Control (ILC) became one of the alternatives to the classical control schemes. It is applied for plants where the control task is executed in finite time horizon trials (or iterations). ILC assumes that in order to improve the control performance and/or quality in the current trial the information gathered from the past is used (Bristow *et al*., 2006; Rogers *et al*., 2023; Dong, 2023; Liu *et al*., 2022). Hence the main idea here is the sequential improvement of the control input defined as the signal applied in the previous trial and the correction term generated basing on the difference between the current plant output and the required reference (so-called the tracking error). The first application of ILC is commonly credited to robotics area where it allowed to improve the robot operation in consecutive executions (Arimoto *et al*., 1984). Such a responsive control strategy was called a robot learning and hence ILC fits into a wide range of techniques generally called a machine learning (Pan and Yang, 2010). Then, due to its potential ILC was used in numerous applications. Among many, control schemes for: robots performing the pick and place tasks (Paszke *et al*., 2013), marine vibrators (Sornmo *et al*., 2016), spatially interconnected systems (Sulikowski *et al*., 2020) or batch processes (Tao *et al*., 2023), ILC proved its applicability and high quality in various cases. Also, some extensions to the basic ILC were proposed regarding, for instance, the application for systems with varying trial lengths (Li *et al*., 2014; Liu and Hou, 2024), control tasks for systems with incomplete information (Shen, 2018) or data-driven only approach (Janssens *et al*., 2013; Yu *et al*., 2021; Dong, 2023).

*Corresponding author

© 2025 M. Pazera et al.
This is an open access article distributed under
the Creative Commons Attribution-NonCommercial-NoDerivs license
(http://creativecommons.org/licenses/by-nc-nd/4.0/).

The main idea of ILC is to improve the control signal across trials. The design process involves selecting past information to generate correction terms and providing appropriate gains to ensure ILC behaves as intended. There are two approaches to determining the correct gains. The first, based on designing $L-$ and $Q-$ filters independently, simplifies the task by allowing separate design procedures (Bristow *et al*., 2006; Bolder *et al*., 2018). The second, the one-stage design, treats the ILC as a subclass of $2D$ systems, specifically Discrete Linear Repetitive Process (DLRP) (Rogers *et al*., 2007), where the so called stability along the trial ensures the convergence of tracking error to zero, driving the system output to the reference signal. Feedback control gains stabilizing the DLRP are then used to design the ILC correction terms.

On the other hand, Fault Tolerant Control (FTC) is a technique for dealing with faults in a system by detecting, isolating, and identifying faults, and using this information to mitigate their negative impact on performance (Saif and Guan, 1993). There are two main FTC approaches (Gao *et al*., 2015). The first is model-based, where system outputs or states are compared with model predictions to detect faults if the residuum is significant. This signal is then used in the feedback control (Witczak, 2007). The second is model-free (data-based), where faults are detected based on prior knowledge and system behavior without a model (Wang and Yang, 2016;2022). Both approaches have their pros and cons.

Additionally, Leal-Leal and Alcorta-Garcia (2023) propose a fault-tolerant controller for nonlinear Euler–Lagrange systems, while Witczak *et al*. (2024) develop a sensor fault diagnosis scheme, and Kukurowski *et al*. (2022) introduce FTC under ellipsoidal bounding. Faults can affect actuators, processes, or sensors, and different approaches are needed for each type. Disturbances and noise, which can cause false alarms, must also be addressed, often using $\mathcal{H}_\infty$ methodology to minimize their influence on the system (Doyle *et al*., 1989).

One notable advantage of ILC is its ability to ensure zero steady-state error. As a result, it can generally be considered a fault-tolerant control scheme. This is because a fault will cause an output deviation, and in subsequent iterations, the control correction will drive this deviation to zero (Rogers *et al*., 2023). However, it is important to note that this property eliminates the fault's influence in future trials, not during the current one. Additionally, while ILC is effective for abrupt faults, it is less efficient for incipient faults. Incipient faults evolve over time, and since ILC requires some trials to adapt the control signal, it may not fully compensate for them. This motivates the integration of ILC with FTC into a single control scheme. The main control objectives are to drive the system to the prescribed reference, minimize or eliminate the effects of disturbances and noise, and compensate for the influence of both abrupt and incipient faults as quickly as possible.

As for the FTC, based on system input and output information, a state and fault observer is implemented and integrated with ILC defined in terms of DLRP. To mitigate the influence of disturbances and noise on the designed scheme, both the fault estimator and the resulting Fault Tolerant Iterative Learning Control (FTILC) scheme utilize the $\mathcal{H}_\infty$ approach. Similar concepts can be found in recent literature (see, e.g., Wang *et al*., 2018; Pazera *et al*., 2021), where actuator faults are considered. In contrast, this paper focuses on possible sensor faults affecting the system.

In this paper, ILC combined with FTC design for the vertical two tank system is developed. In the literature one can find several references devoted to solving problems of that specific class of dynamical systems (Xu *et al*., 2020; Hedrea *et al*., 2019) or systems somehow similar (Zhang *et al*., 2025). Here, in order to model the dynamics, due to the non-linear characteristics of two-tank system considered the Takagi–Sugeno (T–S) system is applied (Takagi and Sugeno, 1985) .

Throughout this paper, $\boldsymbol{M} \succ 0$ ($\boldsymbol{M} \prec 0$) denotes a real symmetric positive (negative) definite matrix, $\boldsymbol{I}$ and $\boldsymbol{0}$ denote, respectively, the identity and zero block matrices of compatible dimensions and $(*)$ denotes symmetric block entries in symmetric matrices.

This paper is organized as follows. Section 2 presents preliminaries and defines the problem of an sensor fault estimation and compensation for Takagi–Sugeno based repetitive systems, Section 3 concerns a proposition for detection and isolation of the sensor fault, while Section 4 is focused on combining FTC and ILC in order to deal with the faults that might appear in some iteration. Section 5 provides the case study with the implementation of the designed FTILC scheme to the two-tank system. Finally, Section 6 provides the results discussion and conclusions.

2. Preliminaries

Let us consider the following nonlinear discrete-time system

$$\boldsymbol{x}_{i,k+1} = f\left(\boldsymbol{x}_{i,k}, \boldsymbol{u}_{i,k}\right), \tag{1}$$

where i stands for the trial (iteration) while k denotes the discrete-time of the i-th iteration. Moreover, $f\left(\cdot\right)$ stands for an unknown nonlinear function which describes the system with respect to the state and input.

Numerous publications (Abonyi and Babuska, 2000; Alexiev and Georgieva, 2004; Deng and Yang, 2016; Li and Fu, 1997) have demonstrated that Takagi–Sugeno models may effectively simulate the aforementioned nonlinear system. The Takagi–Sugeno model can be

reformulated as follows by adding potential sensor fault, external exogenous disturbances, and an output equation:

$$\begin{aligned}\boldsymbol{x}_{i,k+1} &= \boldsymbol{A}\left(\boldsymbol{v}_k\right)\boldsymbol{x}_{i,k} + \boldsymbol{B}\left(\boldsymbol{v}_k\right)\boldsymbol{u}_{i,k} + \boldsymbol{W}_1\boldsymbol{w}_{1,k} \\ &= \sum_{j=1}^{M} h_j\left(\boldsymbol{v}_k\right)\left[\boldsymbol{A}^j\boldsymbol{x}_{i,k} + \boldsymbol{B}^j\boldsymbol{u}_{i,k}\right] + \boldsymbol{W}_1\boldsymbol{w}_{1,k},\end{aligned} \tag{2}$$

$$\boldsymbol{y}_{i,k} = \boldsymbol{C}\boldsymbol{x}_{i,k} + \boldsymbol{C}_f\boldsymbol{f}_{i,k} + \boldsymbol{W}_2\boldsymbol{w}_{2,k}, \tag{3}$$

with

$$h_j(\boldsymbol{v}_k) \geq 0, \quad \forall j = 1, \ldots, M, \quad \sum_{j=1}^{M} h_j(\boldsymbol{v}_k) = 1. \tag{4}$$

Moreover, $\boldsymbol{u}_{i,k} \in \mathbb{R}^r$, $\boldsymbol{y}_{i,k} \in \mathbb{R}^m$, $\boldsymbol{x}_{i,k} \in \mathbb{X} \subset \mathbb{R}^n$ signify input, output and state vectors, respectively. Subsequently, the system matrices are known and given with $\boldsymbol{A}$, $\boldsymbol{B}$ and $\boldsymbol{C}$, where the total amount of subsystems is defined by $\boldsymbol{M}$. Furthermore, a sensor fault vector is defined as $\boldsymbol{f}_{i,k} \in \mathbb{F}_s \subset \mathbb{R}^{n_s}$. Additionally, $\boldsymbol{W}_1$ and $\boldsymbol{W}_2$ stand for the ellipsoidal bounded exogenous external disturbances, which can model several uncertainties, e.g. unmodeled system dynamics, whilst vectors of those uncertainties are given with $\boldsymbol{w}_{1,k}$ and $\boldsymbol{w}_{2,k}$, respectively. Furthermore, $\boldsymbol{v}_k = \left[\boldsymbol{v}_k^1, \boldsymbol{v}_k^2, \ldots, \boldsymbol{v}_k^p\right]^T$ indicates a vector, which contains premise variables as well as depends on measurable variables (Takagi and Sugeno, 1985). Finally, $h_j(\cdot)$ signifies the activation function, which is depending on $\boldsymbol{v}_k$. The last fact implies that it is impossible to estimate more faults than the measured outputs.

Consequently, let us define the following notation $\boldsymbol{A}\left(\boldsymbol{v}_k\right) = \sum_{j=1}^{M} h_j\left(\boldsymbol{v}_k\right)\boldsymbol{A}^j$ where $h_j\left(\boldsymbol{v}_k\right)\boldsymbol{A}^j$ satisfy (4) and describe an equivalent form of the system state equation (2):

$$\boldsymbol{x}_{i,k+1} = \sum_{j=1}^{M} h_j\left(\boldsymbol{v}_k\right)\left[\boldsymbol{A}^j\boldsymbol{x}_{i,k} + \boldsymbol{B}^j\boldsymbol{u}_{i,k}\right] + \boldsymbol{W}_1\boldsymbol{w}_{1,k}, \tag{5}$$

$$\boldsymbol{y}_{i,k} = \boldsymbol{C}\boldsymbol{x}_{i,k} + \boldsymbol{C}_f\boldsymbol{f}_{i,k} + \boldsymbol{W}_2\boldsymbol{w}_{2,k}. \tag{6}$$

For further derivations, let us recall the following lemma (de Oliveira *et al*., 1999):

Lemma 1. *For the matrices $\boldsymbol{V}_i$ and $\boldsymbol{U}$ of appropriate dimensions, the following statements are equivalent:*

1. *There exist $\boldsymbol{X} \succ 0$ and $\boldsymbol{W} \succ 0$ such that*

$$\boldsymbol{V}_i^T\boldsymbol{X}\boldsymbol{V}_i - \boldsymbol{W} \prec 0. \tag{7}$$

2. *There exist $\boldsymbol{X} \succ 0$, $\boldsymbol{W} \succ 0$ and $\boldsymbol{U}$ such that*

$$\begin{bmatrix} -\boldsymbol{W} & \boldsymbol{V}_i^T\boldsymbol{U}^T \\ \boldsymbol{U}\boldsymbol{V}_i & \boldsymbol{X} - \boldsymbol{U} - \boldsymbol{U}^T \end{bmatrix} \prec 0. \tag{8}$$

3. Sensor fault estimation algorithm of a local system

In order to estimate the state and possible sensor faults, the following estimator is applied

$$\begin{aligned}\hat{\boldsymbol{x}}_{i,k+1} &= \boldsymbol{A}(v_k)\hat{\boldsymbol{x}}_{i,k} + \boldsymbol{B}(v_k)\boldsymbol{u}_{i,k} \\ &\quad + \boldsymbol{K}_x\left(\boldsymbol{y}_{i,k} - \boldsymbol{C}\hat{\boldsymbol{x}}_{i,k} - \boldsymbol{C}_f\hat{\boldsymbol{f}}_{i,k}\right),\end{aligned} \tag{9}$$

$$\hat{\boldsymbol{f}}_{i,k+1} = \hat{\boldsymbol{f}}_{i,k} + \boldsymbol{K}_s\left(\boldsymbol{y}_{i,k} - \boldsymbol{C}\hat{\boldsymbol{x}}_{i,k} - \boldsymbol{C}_f\hat{\boldsymbol{f}}_{i,k}\right), \tag{10}$$

where $\hat{\boldsymbol{x}}_{i,k}$ and $\hat{\boldsymbol{f}}_{i,k}$ are state and fault estimates, respectively.

The problem is to determine the gain matrices for the state and fault estimates $\boldsymbol{K}_x$ and $\boldsymbol{K}_s$. To address this problem note that using (2) and (9) the state estimation error can be defined as

$$\begin{aligned}\tilde{\boldsymbol{e}}_{i,k+1} &= \boldsymbol{x}_{i,k+1} - \hat{\boldsymbol{x}}_{i,k+1} = \boldsymbol{A}(v_k)\boldsymbol{x}_{i,k} \\ &\quad + \boldsymbol{B}(v_k)\boldsymbol{u}_{i,k} + \boldsymbol{W}_1\boldsymbol{w}_{1,k} - \boldsymbol{A}(v_k)\hat{\boldsymbol{x}}_{i,k} \\ &\quad - \boldsymbol{B}(v_k)\boldsymbol{u}_{i,k} - \boldsymbol{K}_x\boldsymbol{y}_{i,k} + \boldsymbol{K}_x\boldsymbol{C}\hat{\boldsymbol{x}}_{i,k} \\ &\quad + \boldsymbol{K}_x\boldsymbol{C}_f\hat{\boldsymbol{f}}_{i,k} = \left[\boldsymbol{A}(v_k) - \boldsymbol{K}_x\boldsymbol{C}\right]\tilde{\boldsymbol{e}}_{i,k} \\ &\quad - \boldsymbol{K}_x\boldsymbol{C}_f\boldsymbol{e}_{s,i,k} + \boldsymbol{W}_1\boldsymbol{w}_{1,k} \\ &\quad - \boldsymbol{K}_x\boldsymbol{W}_2\boldsymbol{w}_{2,k},\end{aligned} \tag{11}$$

where $\boldsymbol{e}_{s,i,k} = \boldsymbol{f}_{i,k} - \hat{\boldsymbol{f}}_{i,k}$ is the fault estimation error. Subsequently, using (3) and (10), the fault estimation error can be rewritten as follows

$$\begin{aligned}\boldsymbol{e}_{s,i,k+1} &= \boldsymbol{f}_{i,k+1} - \hat{\boldsymbol{f}}_{i,k+1} = \boldsymbol{f}_{i,k+1} + \boldsymbol{f}_{i,k} \\ &\quad - \boldsymbol{f}_{i,k} - \hat{\boldsymbol{f}}_{i,k} - \boldsymbol{K}_s\boldsymbol{y}_{i,k} + \boldsymbol{K}_s\boldsymbol{C}\hat{\boldsymbol{x}}_{i,k} \\ &\quad + \boldsymbol{K}_s\boldsymbol{C}_f\hat{\boldsymbol{f}}_{i,k} = \boldsymbol{\varepsilon}_k + \left[\boldsymbol{I} - \boldsymbol{K}_s\boldsymbol{C}_f\right]\boldsymbol{e}_{s,i,k} \\ &\quad - \boldsymbol{K}_s\boldsymbol{C}\tilde{\boldsymbol{e}}_{i,k} - \boldsymbol{K}_s\boldsymbol{W}_2\boldsymbol{w}_{2,k},\end{aligned} \tag{12}$$

with $\boldsymbol{\varepsilon}_k = \boldsymbol{f}_{i,k+1} - \boldsymbol{f}_{i,k}$, denoting the fault increment over the following time steps. For the purpose of further analysis it is assumed that $\boldsymbol{\varepsilon}_k \in l_2$. Note that such an assumption is a straightforward consequence of the fact that $\boldsymbol{f}_{i,k+1} \in l_2$ and $\hat{\boldsymbol{f}}_{i,k+1} \in l_2$.

Introduce now the following signals:

$$\bar{\boldsymbol{e}}_{i,k+1} = \begin{bmatrix} \tilde{\boldsymbol{e}}_{i,k+1} \\ \boldsymbol{e}_{s,i,k+1} \end{bmatrix}, \quad \bar{\boldsymbol{w}}_k = \begin{bmatrix} \boldsymbol{w}_{1,k} \\ \boldsymbol{w}_{2,k} \\ \boldsymbol{\varepsilon}_k \end{bmatrix}. \tag{13}$$

Now, it is clear that both the state and fault estimation errors can be presented in a compact form:

$$\begin{aligned}\bar{\boldsymbol{e}}_{i,k+1} &= \boldsymbol{X}(v_k)\bar{\boldsymbol{e}}_{i,k} + \boldsymbol{Z}\bar{\boldsymbol{w}}_k \\ &= (\bar{\boldsymbol{A}}(v_k) - \bar{\boldsymbol{K}}\bar{\boldsymbol{C}})\bar{\boldsymbol{e}}_{i,k} + (\bar{\boldsymbol{W}} - \bar{\boldsymbol{K}}\bar{\boldsymbol{V}})\bar{\boldsymbol{w}}_k,\end{aligned} \tag{14}$$

where

$$\bar{\boldsymbol{A}}(v_k)=\begin{bmatrix}\boldsymbol{A}(v_k) & \boldsymbol{0}\\ \boldsymbol{0} & \boldsymbol{I}\end{bmatrix},\quad \bar{\boldsymbol{C}}=\begin{bmatrix}\boldsymbol{C} & \boldsymbol{I}\end{bmatrix},$$
$$\bar{\boldsymbol{V}}=\begin{bmatrix}\boldsymbol{W}_2 & \boldsymbol{0} & \boldsymbol{0}\end{bmatrix},\quad \bar{\boldsymbol{K}}=\begin{bmatrix}\boldsymbol{K}_x\\ \boldsymbol{K}_s\end{bmatrix},\qquad (15)$$
$$\bar{\boldsymbol{W}}=\begin{bmatrix}\boldsymbol{W}_1 & \boldsymbol{0} & \boldsymbol{0}\\ \boldsymbol{0} & \boldsymbol{0} & \boldsymbol{I}\end{bmatrix}.$$

Remark 1. Note that (14)–(15) can be treated as a discrete system state space model with $\boldsymbol{X}(v_k)$, $\boldsymbol{Z}$ as the closed loop system and external input matrices, respectively. Ensuring stability of that model is equivalent to the convergence to zero (which in fact would denote the correct fault estimation in disturbances present environment) of the proposed scheme (14). Hence the basic idea here is to apply the control design strategy in order to determine gain matrices $\boldsymbol{K}_x$, $\boldsymbol{K}_s$. Note also that the "input" part in (14) is fed by the disturbance / noise signals and it is purposeful to apply the control scheme allowing to mitigate the influence of that part onto the model considered. Hence the $\mathcal{H}_\infty$ technique is proposed to be used in this case. Also, it is to underline that it depends on the observability of (2)–(3). It is important to notice that the possible appearance of sensors faults can negatively influence this feature. What is more, the total failure of ith sensor means that $\boldsymbol{f}_{i,k}=-\boldsymbol{y}_{i,k}$. In such a case the observation matrix $\boldsymbol{C}$ has zero entries in ith row and that in turns devastates the observability of the system. Thus, the performance of the proposed scheme depends on the fact if the system under consideration (2)–(3) is observable even for the fault impaired observation matrix $\boldsymbol{C}$.

Taking into account the estimation error for both state and fault, the following Theorem is proposed:

Theorem 1. *Assume that the faulted system* (2)–(3) *considered is observable. Hence, for a prescribed attenuation level μ_s of $\boldsymbol{v}_k$, the $\mathcal{H}_\infty$ estimator design problem for that system is solvable if there exist matrices $\boldsymbol{N}$, $\boldsymbol{U}$ and $\boldsymbol{P}\succ\boldsymbol{0}$ of an appropriate dimensions such that the following LMI is feasible:*

$$\begin{bmatrix}\boldsymbol{I}-\boldsymbol{P} & \boldsymbol{0} & \boldsymbol{P}_1(v_k)^T\\ \boldsymbol{0} & -\mu_s^2\boldsymbol{I} & \boldsymbol{P}_2(v_k)^T\\ \boldsymbol{P}_1(v_k) & \boldsymbol{P}_2(v_k) & \boldsymbol{P}-\boldsymbol{U}-\boldsymbol{U}^T\end{bmatrix}\prec 0, \qquad (16)$$

where $\boldsymbol{P}_1(v_k)=\boldsymbol{U}\bar{\boldsymbol{A}}(v_k)-\boldsymbol{N}\bar{\boldsymbol{C}}$ and $\boldsymbol{P}_2(v_k)=\boldsymbol{U}\bar{\boldsymbol{W}}-\boldsymbol{N}\bar{\boldsymbol{V}}$. If the LMI of (16) *is feasible, the gain matrices can be computed as*

$$\bar{\boldsymbol{K}}=\begin{bmatrix}\boldsymbol{K}_x\\ \boldsymbol{K}_s\end{bmatrix}=\boldsymbol{U}^{-1}\boldsymbol{N}. \qquad (17)$$

Proof. The problem of designing the $\mathcal{H}_\infty$ observer (Li and Fu, 1997; Zemouche *et al.*, 2008) is to obtain matrices $\boldsymbol{N},\boldsymbol{U}$ and $\boldsymbol{P}$ such that

$$\lim_{k\to\infty}\bar{\boldsymbol{e}}_{i,k}=\boldsymbol{0}\quad\text{for}\quad\bar{\boldsymbol{w}}_k=\boldsymbol{0}, \qquad (18)$$
$$\|\bar{\boldsymbol{e}}_{i,k}\|_{l_2}<\mu_s\|\bar{\boldsymbol{w}}_k\|_{l_2}\quad\text{for}\quad\bar{\boldsymbol{w}}_k\neq\boldsymbol{0},\bar{\boldsymbol{e}}_0=\boldsymbol{0}. \qquad (19)$$

In order to address this issue, it is required to define a Lyapunov function $V_{i,k}$ such that

$$\Delta V_{i,k}+\bar{\boldsymbol{e}}_{i,k}^T\bar{\boldsymbol{e}}_{i,k}-\mu_s^2\bar{\boldsymbol{w}}_k^T\bar{\boldsymbol{w}}_k<0, \qquad (20)$$

where $\Delta V_{i,k}=V_{i,k+1}-V_{i,k}$, $V_{i,k}=\bar{\boldsymbol{e}}_{i,k}^T\boldsymbol{P}\bar{\boldsymbol{e}}_{i,k}$ and $\boldsymbol{P}\succ 0$. If $\bar{\boldsymbol{w}}_k=\boldsymbol{0}$, then the Lyapunov function (20) takes the following simplified form

$$\Delta V_{i,k}+\bar{\boldsymbol{e}}_{i,k}^T\bar{\boldsymbol{e}}_{i,k}<0 \qquad (21)$$

and hence $\Delta V_{i,k}<0$, which leads to (18). If $\bar{\boldsymbol{w}}_k\neq\boldsymbol{0}$ and taking into account the fact that

$$\sum_{k=0}^{\infty}(\Delta V_{i,k})=V_{i,\infty}-V_{i,0},\quad V_{i,\infty}=V_{i,0}=0,$$

then (20) yields:

$$\sum_{k=0}^{\infty}(\Delta V_{i,k})+\sum_{k=0}^{\infty}\left(\bar{\boldsymbol{e}}_{i,k}^T\bar{\boldsymbol{e}}_{i,k}\right)-\mu_s^2\sum_{k=0}^{\infty}\left(\bar{\boldsymbol{w}}_k^T\bar{\boldsymbol{w}}_k\right)<0\Longrightarrow$$
$$-V_0+\sum_{k=0}^{\infty}\left(\bar{\boldsymbol{e}}_{i,k}^T\bar{\boldsymbol{e}}_{i,k}\right)-\mu_s^2\sum_{k=0}^{\infty}\left(\bar{\boldsymbol{w}}_k^T\bar{\boldsymbol{w}}_k\right)<0\Longrightarrow$$
$$\sum_{k=0}^{\infty}\left(\bar{\boldsymbol{e}}_{i,k}^T\bar{\boldsymbol{e}}_{i,k}\right)-\mu_s^2\sum_{k=0}^{\infty}\left(\bar{\boldsymbol{w}}_k^T\bar{\boldsymbol{w}}_k\right)<0\Longrightarrow$$
$$\sum_{k=0}^{\infty}\left(\bar{\boldsymbol{e}}_{i,k}^T\bar{\boldsymbol{e}}_{i,k}\right)<\mu_s^2\sum_{k=0}^{\infty}\left(\bar{\boldsymbol{w}}_k^T\bar{\boldsymbol{w}}_k\right)\Longrightarrow$$
$$\|\bar{\boldsymbol{e}}_{i,k}\|_{l_2}<\mu_s\|\bar{\boldsymbol{w}}_k\|_{l_2},$$

which leads to (19). In what follows, by using (14) it is straightforward to notice that

$$\begin{aligned}\Delta V_{i,k}&+\bar{\boldsymbol{e}}_{i,k}^T\bar{\boldsymbol{e}}_{i,k}-\mu_s^2\bar{\boldsymbol{w}}_k^T\bar{\boldsymbol{w}}_k\\ &=\bar{\boldsymbol{e}}_{i,k}^T\left(\boldsymbol{X}(v_k)^T\boldsymbol{P}\boldsymbol{X}(v_k)+\boldsymbol{I}-\boldsymbol{P}\right)\bar{\boldsymbol{e}}_{i,k}\\ &\quad+\bar{\boldsymbol{e}}_{i,k}^T\left(\boldsymbol{X}(v_k)^T\boldsymbol{P}\boldsymbol{Z}\right)\bar{\boldsymbol{w}}_k\\ &\quad+\bar{\boldsymbol{w}}_k^T\left(\boldsymbol{Z}^T\boldsymbol{P}\boldsymbol{X}(v_k)\right)\bar{\boldsymbol{e}}_{i,k}\\ &\quad+\bar{\boldsymbol{w}}_k^T\left(\boldsymbol{Z}^T\boldsymbol{P}\boldsymbol{Z}-\mu_s^2\boldsymbol{I}\right)\bar{\boldsymbol{w}}_k<0.\end{aligned} \qquad (22)$$

Now introduce

$$\bar{\boldsymbol{v}}_{i,k}=\begin{bmatrix}\bar{\boldsymbol{e}}_{i,k}\\ \bar{\boldsymbol{w}}_k\end{bmatrix}, \qquad (23)$$

and it leads to the fact that (22) can be rewritten as

$$\bar{\boldsymbol{v}}_{i,k}^T\begin{bmatrix}\boldsymbol{X}(v_k)^T\boldsymbol{P}\boldsymbol{X}(v_k)+\boldsymbol{I}-\boldsymbol{P} & \boldsymbol{X}(v_k)^T\boldsymbol{P}\boldsymbol{Z}\\ \boldsymbol{Z}^T\boldsymbol{P}\boldsymbol{X}(v_k) & \boldsymbol{Z}^T\boldsymbol{P}\boldsymbol{Z}-\mu_s^2\boldsymbol{I}\end{bmatrix}\times\bar{\boldsymbol{v}}_{i,k}\prec 0, \qquad (24)$$

which is equivalent to

$$\begin{bmatrix} \boldsymbol{X}(v_k)^T \\ \boldsymbol{Z}^T \end{bmatrix} \boldsymbol{P} \begin{bmatrix} \boldsymbol{X}(v_k) & \boldsymbol{Z} \end{bmatrix} + \begin{bmatrix} \boldsymbol{I}-\boldsymbol{P} & \boldsymbol{0} \\ \boldsymbol{0} & -\mu_s^2 \boldsymbol{I} \end{bmatrix} \prec 0. \tag{25}$$

Applying Lemma 1 to (25) provides

$$\begin{bmatrix} \boldsymbol{I}-\boldsymbol{P} & \boldsymbol{0} & \boldsymbol{X}(v_k)^T \boldsymbol{U}^T \\ \boldsymbol{0} & -\mu_s^2 \boldsymbol{I} & \boldsymbol{Z}^T \boldsymbol{U}^T \\ \boldsymbol{U}\boldsymbol{X}(v_k) & \boldsymbol{U}\boldsymbol{Z} & \boldsymbol{P}-\boldsymbol{U}-\boldsymbol{U}^T \end{bmatrix} \prec 0 \tag{26}$$

and then after applying the following

$$\begin{aligned} \boldsymbol{U}\boldsymbol{X}(v_k) &= \boldsymbol{U}\bar{\boldsymbol{A}}(v_k) - \boldsymbol{U}\bar{\boldsymbol{K}}\bar{\boldsymbol{C}} \\ &= \boldsymbol{U}\bar{\boldsymbol{A}}(v_k) - \boldsymbol{N}\bar{\boldsymbol{C}}, \end{aligned} \tag{27}$$

$$\boldsymbol{U}\boldsymbol{Z} = \boldsymbol{U}\bar{\boldsymbol{W}} - \boldsymbol{U}\bar{\boldsymbol{K}}\bar{\boldsymbol{V}} = \boldsymbol{U}\bar{\boldsymbol{W}} - \boldsymbol{N}\bar{\boldsymbol{V}} \tag{28}$$

leads to (16), which completes the proof. ■

4. Integrated fault-tolerant iterative learning control design

The objective of this section is to utilize FTC and integrate it with ILC. Therefore, let us define a fault-tolerant ILC input as

$$\boldsymbol{u}_{i+1,k} = \boldsymbol{u}_{i,k} + \Delta\boldsymbol{u}_{i+1,k}, \tag{29}$$

where $\Delta\boldsymbol{u}_{i+1,k}$ represents a correction term. It is clear now that the control signal in the following trial is defined as a control input from the current trial improved by a part that is related to the current trial difference between the output and the prescribed reference. Since the application of ILC provides the ability to get rid of the steady state error in general, it might be treated as a fault tolerant control scheme. However, it needs to be underlined that this property will allow to eliminate the influence of the fault in following trials. Also, it will work efficiently for the abrupt faults, however not so successfully for the incipient ones. Nevertheless, ILC does not ensure compensation for the sensor fault in the ith iteration. Furthermore, if the sensor fault remains uncompensated in the current iteration, the deviation between the current and expected signals will be utilized to calculate control for future trials. To prevent this scenario, the FTC scheme is merged with ILC. The goal is to minimize the tracking error over the trials

$$\boldsymbol{e}_{i+1,k} = \boldsymbol{y}_{r,k} - \boldsymbol{y}_{i+1,k}, \tag{30}$$

where $\boldsymbol{y}_{r,k}$ stands for a reference signal. The tracking error can also be perceived as

$$\boldsymbol{e}_{i+1,k} = \boldsymbol{y}_{r,k} - \boldsymbol{C}\boldsymbol{x}_{i+1,k} - \boldsymbol{C}_f\boldsymbol{f}_{i+1,k} - \boldsymbol{W}_2\boldsymbol{w}_{2,k}. \tag{31}$$

We shall introduce

$$\eta_{i+1,k} = \boldsymbol{x}_{i+1,k-1} - \boldsymbol{x}_{i,k-1}, \tag{32}$$

standing for an error of the consecutive iterations. Next, by substituting (2)–(3) and (29) into (30), we can demonstrate that

$$\begin{aligned} \boldsymbol{e}_{i+1,k} - \boldsymbol{e}_{i,k} = &-\boldsymbol{C}\boldsymbol{x}_{i+1,k} - \boldsymbol{C}_f\boldsymbol{f}_{i+1,k} \\ &- \boldsymbol{W}_2\boldsymbol{w}_{2,k} + \boldsymbol{C}\boldsymbol{x}_{i,k} + \boldsymbol{C}_f\boldsymbol{f}_{i,k} \\ &+ \boldsymbol{W}_2\boldsymbol{w}_{2,k}. \end{aligned} \tag{33}$$

Assuming that the measurement uncertainty vector $\boldsymbol{w}_{2,k}$ is constant at i, then (33) reduces to

$$\begin{aligned} \boldsymbol{e}_{i+1,k} - \boldsymbol{e}_{i,k} = &-\boldsymbol{C}\boldsymbol{x}_{i+1,k} - \boldsymbol{C}_f\boldsymbol{f}_{i+1,k} + \boldsymbol{C}\boldsymbol{x}_{i,k} \\ &+ \boldsymbol{C}_f\boldsymbol{f}_{i,k}. \end{aligned} \tag{34}$$

Thus,

$$\begin{aligned} \boldsymbol{e}_{i+1,k} = &\boldsymbol{e}_{i,k} - \boldsymbol{C}\boldsymbol{x}_{i+1,k} - \boldsymbol{C}_f\boldsymbol{f}_{i+1,k} + \boldsymbol{C}\boldsymbol{x}_{i,k} \\ &+ \boldsymbol{C}_f\boldsymbol{f}_{i,k} = \boldsymbol{e}_{i,k} - \boldsymbol{C}\boldsymbol{A}(\boldsymbol{v}_k)\boldsymbol{x}_{i+1,k-1} \\ &- \boldsymbol{C}\boldsymbol{B}(\boldsymbol{v}_k)\boldsymbol{u}_{i+1,k-1} - \boldsymbol{C}_f\boldsymbol{f}_{i+1,k} \\ &+ \boldsymbol{C}\boldsymbol{A}(\boldsymbol{v}_k)\boldsymbol{x}_{i,k-1} + \boldsymbol{C}\boldsymbol{B}(\boldsymbol{v}_k)\boldsymbol{u}_{i,k-1} \\ &+ \boldsymbol{C}_f\boldsymbol{f}_{i,k}. \end{aligned} \tag{35}$$

From (29) it is evident that

$$\Delta\boldsymbol{u}_{i+1,k} = \boldsymbol{u}_{i+1,k} - \boldsymbol{u}_{i,k}. \tag{36}$$

Similarly, we propose

$$\Delta\boldsymbol{f}_{i+1,k} = \boldsymbol{f}_{i+1,k} - \boldsymbol{f}_{i,k}. \tag{37}$$

Applying (29) and (32) as well as (36)–(37) yields

$$\begin{aligned} \boldsymbol{e}_{i+1,k} = &\boldsymbol{e}_{i,k} - \boldsymbol{C}\boldsymbol{A}(\boldsymbol{v}_k)\eta_{i+1,k} \\ &- \boldsymbol{C}\boldsymbol{B}(\boldsymbol{v}_k)\boldsymbol{u}_{i+1,k-1} + \boldsymbol{C}\boldsymbol{B}(\boldsymbol{v}_k)\boldsymbol{u}_{i,k-1} \\ &- \boldsymbol{C}_f\boldsymbol{f}_{i+1,k} + \boldsymbol{C}_f\boldsymbol{f}_{i,k} = \boldsymbol{e}_{i,k} \\ &- \boldsymbol{C}\boldsymbol{A}(\boldsymbol{v}_k)\eta_{i+1,k} - \boldsymbol{C}_f\Delta\boldsymbol{f}_{i+1,k} \\ &- \boldsymbol{C}\boldsymbol{B}(\boldsymbol{v}_k)\Delta\boldsymbol{u}_{i+1,k-1}. \end{aligned} \tag{38}$$

Let us establish

$$\Delta\boldsymbol{u}_{i+1,k} = \boldsymbol{K}_1\eta_{i+1,k+1} + \boldsymbol{K}_2\boldsymbol{e}_{i,k+1}. \tag{39}$$

In addition, the subsequent dynamics can be formulated as

$$\begin{aligned} \eta_{i+1,k+1} = \boldsymbol{x}_{i+1,k} - \boldsymbol{x}_{i,k} = &\boldsymbol{A}(\boldsymbol{v}_k)\eta_{i+1,k} \\ &+ \boldsymbol{B}(\boldsymbol{v}_k)\Delta\boldsymbol{u}_{i+1,k} = \boldsymbol{H}(\boldsymbol{v}_k)\eta_{i+1,k} \\ &+ \boldsymbol{B}(\boldsymbol{v}_k)\boldsymbol{K}_2\boldsymbol{e}_{i,k}, \end{aligned} \tag{40}$$

where $\boldsymbol{H}(\boldsymbol{v}_k) = (\boldsymbol{A}(\boldsymbol{v}_k) + \boldsymbol{B}(\boldsymbol{v}_k)\boldsymbol{K}_1)$.

We introduce

$$\zeta_{i+1,k+1} = \hat{\boldsymbol{x}}_{i+1,k} - \hat{\boldsymbol{x}}_{i,k}. \tag{41}$$

Remark 2. Please note that this is the climax of the paper, namely the combination of the ILC and FTC strategies. This is accomplished in such a way that the control is based on the state estimate, which is fault-free (due to the specific structure of the estimator), rather than the actual state, or more specifically, the output signal containing the sensor faults.

Taking into account that $\hat{\boldsymbol{x}}_{i,k} = \boldsymbol{x}_{i,k} - \tilde{\boldsymbol{e}}_{i,k}$ hence, $\boldsymbol{x}_{i,k} = \hat{\boldsymbol{x}}_{i,k} + \tilde{\boldsymbol{e}}_{i,k}$, it can be shown that

$$\begin{aligned}\zeta_{i+1,k+1} &= \hat{\boldsymbol{x}}_{i+1,k} + \tilde{\boldsymbol{e}}_{i+1,k} - \hat{\boldsymbol{x}}_{i,k} - \tilde{\boldsymbol{e}}_{i,k}\\ &= \boldsymbol{A}(\boldsymbol{v}_k)\hat{\boldsymbol{x}}_{i+1,k-1} + \boldsymbol{B}(\boldsymbol{v}_k)\boldsymbol{u}_{i+1,k-1}\\ &\quad + \boldsymbol{K}_x\left(\boldsymbol{y}_{i+1,k-1} - \boldsymbol{C}\hat{\boldsymbol{x}}_{i+1,k-1}\right.\\ &\quad \left.-\boldsymbol{C}_f\hat{\boldsymbol{f}}_{i+1,k-1}\right) + \tilde{\boldsymbol{e}}_{i+1,k}\\ &\quad - \boldsymbol{K}_x\left(\boldsymbol{y}_{i,k-1} - \boldsymbol{C}\hat{\boldsymbol{x}}_{i,k-1} - \boldsymbol{C}_f\hat{\boldsymbol{f}}_{i,k-1}\right)\\ &\quad - \boldsymbol{A}(\boldsymbol{v}_k)\hat{\boldsymbol{x}}_{i,k-1} - \boldsymbol{B}(\boldsymbol{v}_k)\boldsymbol{u}_{i,k-1} + \tilde{\boldsymbol{e}}_{i,k}\\ &= \boldsymbol{A}(\boldsymbol{v}_k)\zeta_{i+1,k} + \boldsymbol{B}(\boldsymbol{v}_k)\Delta\boldsymbol{u}_{i+1,k-1}\\ &\quad + \boldsymbol{K}_x\boldsymbol{C}\tilde{\boldsymbol{e}}_{i+1,k-1} - \boldsymbol{K}_x\boldsymbol{C}\tilde{\boldsymbol{e}}_{i,k-1}\\ &\quad + \boldsymbol{K}_x\boldsymbol{C}_f\boldsymbol{e}_{s,i+1,k-1} - \boldsymbol{K}_x\boldsymbol{C}_f\boldsymbol{e}_{s,i,k-1},\end{aligned} \tag{42}$$

which brings

$$\begin{aligned}\zeta_{i+1,k+1} &= \boldsymbol{A}(\boldsymbol{v}_k)\zeta_{i+1,k} + \boldsymbol{B}(\boldsymbol{v}_k)\boldsymbol{K}_1\zeta_{i+1,k}\\ &\quad + \boldsymbol{B}(\boldsymbol{v}_k)\boldsymbol{K}_2\boldsymbol{e}_{i,k} + \boldsymbol{K}_x\boldsymbol{C}\tilde{\boldsymbol{e}}_{i+1,k-1}\\ &\quad - \boldsymbol{K}_x\boldsymbol{C}\tilde{\boldsymbol{e}}_{i,k-1} + \boldsymbol{K}_x\boldsymbol{C}_f\boldsymbol{e}_{s,i+1,k-1}\\ &\quad - \boldsymbol{K}_x\boldsymbol{C}_f\boldsymbol{e}_{s,i,k-1}.\end{aligned} \tag{43}$$

Hence,

$$\begin{aligned}\boldsymbol{e}_{i+1,k} &= \boldsymbol{e}_{i,k} - \boldsymbol{G}(\boldsymbol{v}_k)\zeta_{i+1,k} - \boldsymbol{G}(\boldsymbol{v}_k)\tilde{\boldsymbol{e}}_{i+,k-1}\\ &\quad - \boldsymbol{M}(\boldsymbol{v}_k)\Delta\boldsymbol{u}_{i+1,k-1} + \boldsymbol{G}(\boldsymbol{v}_k)\tilde{\boldsymbol{e}}_{i,k-1}\\ &\quad - \boldsymbol{C}_f\Delta\boldsymbol{f}_{i+1,k} = \boldsymbol{e}_{i,k} - \boldsymbol{G}(\boldsymbol{v}_k)\zeta_{i+1,k}\\ &\quad - \boldsymbol{G}(\boldsymbol{v}_k)\tilde{\boldsymbol{e}}_{i+,k-1} - \boldsymbol{C}_f\Delta\boldsymbol{f}_{i+1,k}\\ &\quad - \boldsymbol{M}(\boldsymbol{v}_k)\boldsymbol{K}_1\zeta_{i+1,k} - \boldsymbol{M}(\boldsymbol{v}_k)\boldsymbol{K}_2\boldsymbol{e}_{i,k}\\ &\quad + \boldsymbol{G}(\boldsymbol{v}_k)\tilde{\boldsymbol{e}}_{i,k-1},\end{aligned} \tag{44}$$

where $\boldsymbol{G}(\boldsymbol{v}_k) = \boldsymbol{C}\boldsymbol{A}(\boldsymbol{v}_k)$ and $\boldsymbol{M}(\boldsymbol{v}_k) = \boldsymbol{C}\boldsymbol{B}(\boldsymbol{v}_k)$.

Thus, the controlled sensor FTILC dynamics can be written as

$$\begin{aligned}\begin{bmatrix}\begin{bmatrix}\zeta_{i+1,k+1}\\ \boldsymbol{e}_{i+1,k}\end{bmatrix}\\ \bar{\boldsymbol{e}}_{i+1,k}\\ \bar{\boldsymbol{e}}_{i,k}\end{bmatrix} &= \left[\begin{array}{c|c}\bar{\boldsymbol{A}}_1(\boldsymbol{v}_k) & \bar{\boldsymbol{A}}_2(\boldsymbol{v}_k)\\ \hline \bar{\boldsymbol{A}}_3(\boldsymbol{v}_k) & \bar{\boldsymbol{A}}_4(\boldsymbol{v}_k)\end{array}\right]\\ &\quad\times\begin{bmatrix}\begin{bmatrix}\zeta_{i+1,k}\\ \boldsymbol{e}_{i,k}\end{bmatrix}\\ \bar{\boldsymbol{e}}_{i+1,k-1}\\ \bar{\boldsymbol{e}}_{i,k-1}\end{bmatrix} + \begin{bmatrix}\begin{bmatrix}0 & 0\\ 0 & 0\end{bmatrix}\\ \begin{bmatrix}\boldsymbol{Z} & \boldsymbol{0}\\ \boldsymbol{0} & \boldsymbol{Z}\end{bmatrix}\end{bmatrix}\\ &\quad\times\begin{bmatrix}\bar{\boldsymbol{w}}_{i+1,k-1}\\ \bar{\boldsymbol{w}}_{i,k-1}\end{bmatrix},\end{aligned} \tag{45}$$

where

$$\begin{aligned}\bar{\boldsymbol{A}}_1(\boldsymbol{v}_k) &= \begin{bmatrix}\boldsymbol{A}_1(\boldsymbol{v}_k) & \boldsymbol{A}_2(\boldsymbol{v}_k)\\ \boldsymbol{A}_3(\boldsymbol{v}_k) & \boldsymbol{A}_4(\boldsymbol{v}_k)\end{bmatrix},\\ \bar{\boldsymbol{A}}_2(\boldsymbol{v}_k) &= \begin{bmatrix}\tilde{\boldsymbol{B}}(\boldsymbol{v}_k) & \tilde{\boldsymbol{B}}(\boldsymbol{v}_k)\\ \tilde{\boldsymbol{C}}(\boldsymbol{v}_k) & \tilde{\boldsymbol{C}}(\boldsymbol{v}_k)\end{bmatrix},\\ \bar{\boldsymbol{A}}_3(\boldsymbol{v}_k) &= \begin{bmatrix}\boldsymbol{0} & \boldsymbol{0}\\ \boldsymbol{0} & \boldsymbol{0}\end{bmatrix},\\ \bar{\boldsymbol{A}}_4(\boldsymbol{v}_k) &= \begin{bmatrix}\boldsymbol{X}(\boldsymbol{v}_k) & \boldsymbol{0}\\ \boldsymbol{0} & \boldsymbol{X}(\boldsymbol{v}_k)\end{bmatrix},\\ \boldsymbol{A}_1(\boldsymbol{v}_k) &= \boldsymbol{A}(\boldsymbol{v}_k) + \boldsymbol{B}(\boldsymbol{v}_k)\boldsymbol{K}_1,\\ \boldsymbol{A}_2(\boldsymbol{v}_k) &= \boldsymbol{B}(\boldsymbol{v}_k)\boldsymbol{K}_2,\\ \boldsymbol{A}_3(\boldsymbol{v}_k) &= -\boldsymbol{C}\boldsymbol{A}(\boldsymbol{v}_k) - \boldsymbol{C}\boldsymbol{B}(\boldsymbol{v}_k)\boldsymbol{K}_1,\\ \boldsymbol{A}_4(\boldsymbol{v}_k) &= -\boldsymbol{C}\boldsymbol{B}(\boldsymbol{v}_k)\boldsymbol{K}_2.\end{aligned}$$

In this instance, Eqn. (45) can be thought of as an upper block triangular matrix, in which the blocks on the diagonal alone define the eigenvalues of the extended system. It follows that separate design of the fault estimator and ILC controller is possible. In light of this, the ILC dynamics can be recast as the subsequent iterative process:

$$\begin{bmatrix}\zeta_{i+1,k+1}\\ \boldsymbol{e}_{i+1,k}\end{bmatrix} = \begin{bmatrix}\boldsymbol{A}_1(\boldsymbol{v}_k) & \boldsymbol{A}_2(\boldsymbol{v}_k)\\ \boldsymbol{A}_3(\boldsymbol{v}_k) & \boldsymbol{A}_4(\boldsymbol{v}_k)\end{bmatrix}\begin{bmatrix}\zeta_{i+1,k}\\ \boldsymbol{e}_{i,k}\end{bmatrix}. \tag{46}$$

Consequently, it was shown that the discrete linear repetitive process can be used to characterize the FTILC scheme (see the work of Rogers *et al*. (2007) and the references therein). Furthermore, for such a system, proving stability along the trial also demonstrates that the underlying ILC converges to zero and that the intended reference is reached.

Theorem 2. (Rogers *et al.*, 2007) *The sensor FTILC scheme defined in terms of the discrete linear repetitive process* (46)*, is stable along the trial if there exist dimension-compatible matrices* $\boldsymbol{P} = diag(\boldsymbol{P}_1, \boldsymbol{P}_2) \succ 0$ *and* $\boldsymbol{N}_1$*,* $\boldsymbol{N}_2$ *such that the following LMI is feasible*

$$\begin{bmatrix}-\boldsymbol{P} & \boldsymbol{P}\Gamma(\boldsymbol{v}_k)^T + \boldsymbol{N}^T\Omega(\boldsymbol{v}_k)^T\\ \boldsymbol{P}\Gamma(\boldsymbol{v}_k) + \Omega(\boldsymbol{v}_k)\boldsymbol{N} & -\boldsymbol{P}\end{bmatrix} \prec 0, \tag{47}$$

where

$$\begin{aligned}\Gamma(\boldsymbol{v}_k) &= \begin{bmatrix}\boldsymbol{A}(\boldsymbol{v}_k) & \boldsymbol{0}\\ -\boldsymbol{C}\boldsymbol{A}(\boldsymbol{v}_k) & \boldsymbol{I}\end{bmatrix},\\ \boldsymbol{N} &= \begin{bmatrix}\boldsymbol{N}_1 & \boldsymbol{N}_2\\ \boldsymbol{N}_1 & \boldsymbol{N}_2\end{bmatrix},\\ \Omega(\boldsymbol{v}_k) &= \begin{bmatrix}\boldsymbol{B}(\boldsymbol{v}_k) & \boldsymbol{0}\\ \boldsymbol{0} & -\boldsymbol{C}\boldsymbol{B}(\boldsymbol{v}_k)\end{bmatrix}.\end{aligned}$$

If the LMI (47) is feasible, the gain matrices for the FTILC controller are given by

$$\begin{aligned}\boldsymbol{K}_1 &= \boldsymbol{N}_1\boldsymbol{P}_1^{-1},\\ \boldsymbol{K}_2 &= \boldsymbol{N}_2\boldsymbol{P}_2^{-1}.\end{aligned} \tag{48}$$

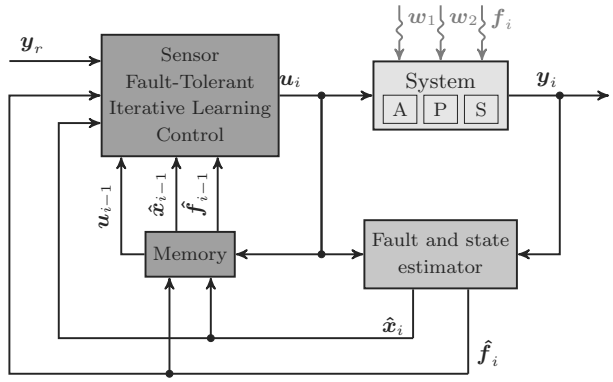


Fig. 1. Block diagram of the proposed sensor fault-tolerant iterative learning control.

Remark 3. Please take note that the controller design procedure (47) and the estimation design procedure (16) can be expressed simply as suitable sets of $\boldsymbol{M}$ LMIs corresponding to all vertices shaping (5). Therefore, the problem reduces to solving the set of LMIs (47) and (16) for the controller and estimator, respectively, and then utilizing (17) and (48) to determine the appropriate gain matrices.

It is worth to highlighting that, in the case of a DLRP, when the required property is guaranteed by appropriate feedback-based control, an examination of (46) would lead to an approaching zero tracking output error $\boldsymbol{e}_{i,k}$ in terms of ILC. As a result, this would suggest that the reference signal $\boldsymbol{y}_{r,k}$ is reached by the system output, (3).

The proposed FTILC approach capable of compensating sensor faults can be summarized using the block diagram presented in Fig. 1. It should be pointed out that in this scheme the sensor fault estimate is included in the state estimate, which results with the state estimate free from sensor faults. That scheme clearly illustrates the flow of the signals in the proposed approach.

5. Case study

Examining a two-tank system (shown in Fig. 2) can help to demonstrate how successful the designed methodology is. The two separate tanks that make up this system are stacked vertically, one on the top of the other. It also has two pumps; the upper pump fills the upper tank and the lower pump fills the lower tank with water. Gravity pulls the water out of these tanks and the fluid pulled out from the higher tank supplies the lower one simultaneously with the pump. In the state-space representation, the mathematical model of the system takes the specific form



Fig. 2. Two-tank system.

of (1) and is given as

$$\boldsymbol{x}_{i,k+1} = \boldsymbol{A}_c\boldsymbol{x}_{i,k} + \boldsymbol{B}_c\boldsymbol{u}_{i,k} + \boldsymbol{W}_1\boldsymbol{w}_{1,k}, \tag{49}$$

$$\boldsymbol{y}_{i,k} = \boldsymbol{C}\boldsymbol{x}_{i,k} + \boldsymbol{C}_f\boldsymbol{f}_{i,k} + \boldsymbol{W}_2\boldsymbol{w}_{2,k}, \tag{50}$$

where

$$\boldsymbol{A}_c = \begin{bmatrix} \frac{-K}{2F_m\sqrt{h_1}} & 0 \\ \frac{K}{2F_m\sqrt{h_1}} & \frac{-K}{2F_m\sqrt{h_2}} \end{bmatrix}, \quad \boldsymbol{B}_c = \begin{bmatrix} \frac{1}{F} & 0 \\ 0 & \frac{1}{F} \end{bmatrix}, \tag{51}$$

and $\boldsymbol{x} = [h_1,\, h_2]^T$ stands for the state composing of the liquid levels in the respective tanks. Since both states are measured, $\boldsymbol{C}$ is an identity matrix. The rest of matrices and signals have the meaning defined for (5)–(6). The flow constant is $K = 0.85\ [\sqrt{m^5}/s]$ and the cross-section area is $F_m = 3.6\ [m^2]$. It is to be noted that due to the structure of $\boldsymbol{A}_c$, (49)–(50) is nonlinear.

In what follows (49)–(50) has been modeled in the form of a T–S system given by (5)–(6), with the following matrices (provided upon considered system's rank and its nonlinear behavior)

$$\boldsymbol{A}^1 = \begin{bmatrix} 0.8397 & 0.0000 \\ -0.0318 & 0.8397 \end{bmatrix}, \quad \boldsymbol{A}^2 = \begin{bmatrix} 0.8397 & 0.0000 \\ -0.0318 & 1.0264 \end{bmatrix},$$

$$\boldsymbol{A}^3 = \begin{bmatrix} 0.8397 & 0.0000 \\ 0.1549 & 0.8397 \end{bmatrix}, \quad \boldsymbol{A}^4 = \begin{bmatrix} 0.8397 & 0.0000 \\ 0.1549 & 1.0264 \end{bmatrix},$$

$$\boldsymbol{A}^5 = \begin{bmatrix} 1.0264 & 0.0000 \\ -0.0318 & 0.8397 \end{bmatrix}, \quad \boldsymbol{A}^6 = \begin{bmatrix} 1.0264 & 0.0000 \\ -0.0318 & 1.0264 \end{bmatrix},$$

$$\boldsymbol{A}^7 = \begin{bmatrix} 1.0264 & 0.0000 \\ 0.1549 & 0.8397 \end{bmatrix}, \quad \boldsymbol{A}^8 = \begin{bmatrix} 1.0264 & 0.0000 \\ 0.1549 & 1.0264 \end{bmatrix},$$

$$\boldsymbol{B}^j = \begin{bmatrix} 0.2534 & 0.0000 \\ 0.0229 & 0.2534 \end{bmatrix}, \qquad j = 1 \ldots 8.$$

Table 1. Fault scenario F-Sc-1 performed during the experiment.

Fault	Magnitude	Time of fault occurrence
$\boldsymbol{f}_{1,i,k}$	-0.15	$k > 40$
$\boldsymbol{f}_{2,i,k}$	-0.25	$60 > k > 80$

for $i = 12$.

Table 2. Fault scenario F-Sc-2 performed during the experiment.

Fault	Magnitude	Time of fault occurrence
$\boldsymbol{f}_{1,i,k}$	-0.14	$40 > k > 60$
$\boldsymbol{f}_{1,i,k}$	-0.12	$61 > k > 80$
$\boldsymbol{f}_{1,i,k}$	-0.1	$81 > k > 100$
$\boldsymbol{f}_{1,i,k}$	-0.08	$101 > k > 120$
$\boldsymbol{f}_{1,i,k}$	-0.06	$121 > k > 140$
$\boldsymbol{f}_{1,i,k}$	-0.04	$141 > k > 160$
$\boldsymbol{f}_{1,i,k}$	-0.02	$161 > k > 180$
$\boldsymbol{f}_{1,i,k}$	0	otherwise
$\boldsymbol{f}_{2,i,k}$	0	

for $i = 12$.

It's also critical to remember that during the experiments, all outputs were measured, yielding the finding $\boldsymbol{C} = \boldsymbol{I}_{m\times m},\ m = 2$.

Disturbance and noise distribution matrices have been assumed as $\boldsymbol{W}_1 = \text{diag}(0.1, 0.1)$, $\boldsymbol{W}_2 = \text{diag}(0.01, 0.01)$, and finally, the fault influence matrix $\boldsymbol{C}_f = \boldsymbol{C}$. The vectors $\boldsymbol{w}_{1,k}$ and $\boldsymbol{w}_{2,k}$ are generated according to the truncated normal distribution with the expected value equal to 0, standard deviation $\sigma_w = 0.0577$ and $\sigma_v = 0.1030$ and the truncation level equal to $4 \cdot 10^{-4}$ and $2 \cdot 10^{-4}$, respectively.

A fault scenario was studied in order to assess the efficacy of the suggested approach with regard to fault estimation and fault-tolerant control. Table 2 contains the details of that fault scenario.

It is evident from the table that faults of different sizes were taken into account. A sensor malfunction of 0 denotes a situation in which there are no defects. Any other value indicates the opposite. These numbers, which are given in $[m]$, represent the offset of the liquid level in the tanks from their actual value. Measured from the beginning of the experiment, the faults were introduced at a predetermined time of $40[s]$ for the first sensor and $60[s]$ for the second. It can also be noticed that the fault of the first sensor has a constant nature, which means that once it occurs, it remains until the end of the repetition. However, the fault of the second sensor is temporary and lasts only for 20 seconds. Reaching and maintaining predetermined water levels in each tank was the control's goal during these testing; the target levels were established as the control aim, which can be observed in Fig. 3 for the top tank and the lower tank, respectively.

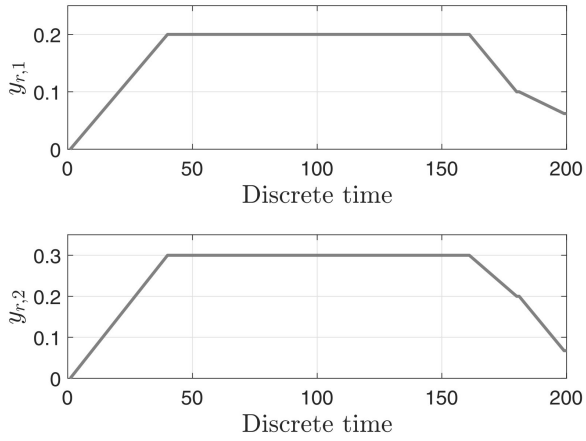


Fig. 3. References for each tank.

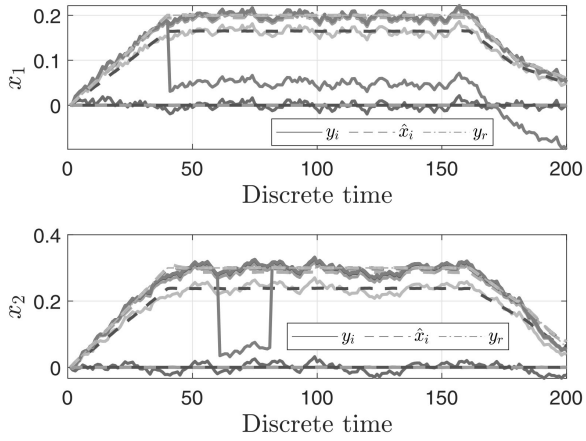


Fig. 4. State evolution over the trials.

After solving the set of LMIs responsible for designing the state and fault estimator (16) as well as the controller (47), the following gain matrices have been obtained:

$$\begin{aligned}
\boldsymbol{K}_x &= \begin{bmatrix} 0.0385 & -0.0028 \\ -0.0605 & 0.0047 \end{bmatrix}, \\
\boldsymbol{K}_s &= \begin{bmatrix} 0.9356 & 0.0010 \\ 0.0753 & 0.9779 \end{bmatrix}, \\
\boldsymbol{K}_1 &= \begin{bmatrix} -3.0595 & 0.2171 \\ -0.0952 & -3.0523 \end{bmatrix}, \\
\boldsymbol{K}_2 &= \begin{bmatrix} 2.0763 & 0.0247 \\ -0.1554 & 2.0820 \end{bmatrix}.
\end{aligned} \tag{52}$$

Figure 4 presents the state evolution over the repetitions for both the upper and lower tanks. It can be easily seen that the states tend to the references, reducing the error with each repetition. The tracking error converges to the reference within 5 and 4 repetitions for the upper and lower tanks, respectively, with the error

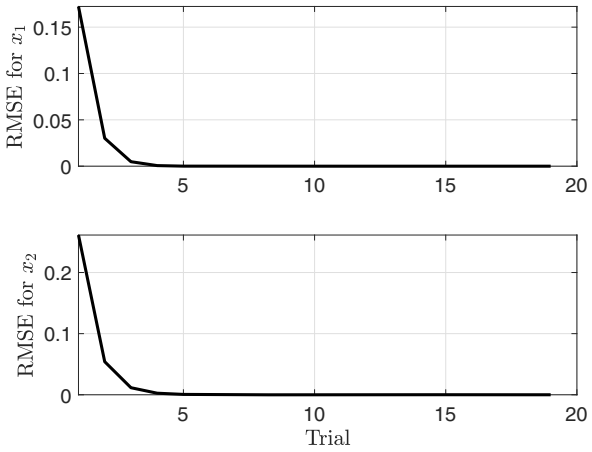


Fig. 5. RMSE evolution.

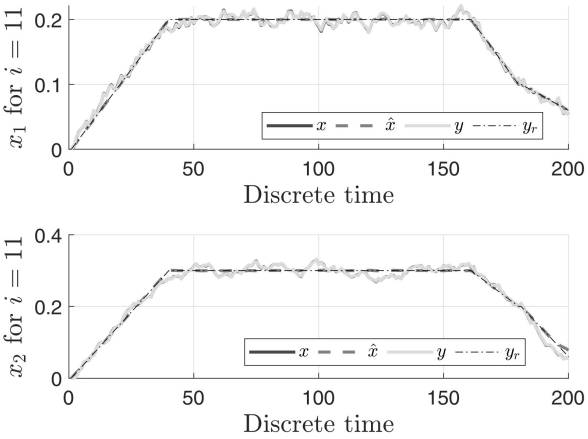


Fig. 6. Results for $i = 11$.

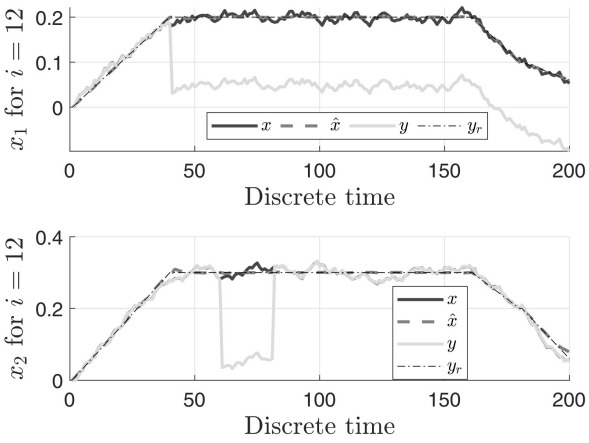


Fig. 7. Results for $i = 12$.

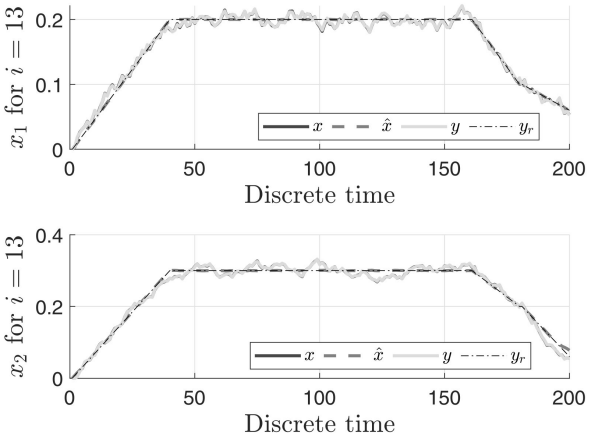


Fig. 8. Results for $i = 13$.

being less than 3%. The root mean square error for each repetition is portrayed in Fig. 5. It clearly shows that the output is getting closer to the reference with each iteration.

During the experiments, it was assumed that the sensor faults in the upper and lower tanks occur in the repetition $i = 12$. For clarity of presentation and to demonstrate that the proposed FTILC strategy compensates for the occurring sensor faults in the current iteration, furthermore, the impact of the faults is not considered when calculating control for subsequent trials. Taking this into account, Figs. 6–8 show the system's responses for three consecutive repetitions, starting from $i = 11$ and continuing through $i = 13$. From these figures, it is evident that the proposed strategy meets the aforementioned assumptions. The state has been following the reference despite the sensor faults. This situation arises because the state estimates follow the actual states, regardless of faulty output.

The quality of the sensor FTILC control is strongly associated with the quality of the sensor fault estimate. Figures 9–10 present the sensor fault estimate for both the upper and lower tank in the faulty repetition as well as in the one fault-free arbitrarily selected iteration.

From these figures it can be noticed that the sensor faults were reconstructed with a very good precision.

The last but not least it is worth to mention of the control inputs calculated within the proposed approach. The evolution of the control for both pumps along all the trials is presented in Fig. 11. It can be easily noticed that in each trial the control has been adapted to the initial conditions being the control from previous trial which results with increasing the quality of control over the trials.

To verify to which fault magnitude the proposed algorithm is able to isolate the sensor fault properly, the fault scenario F-Sc-2 (see Table 2) has been provided.

In this scenario, the fault appears in time instance $k = 20$ with magnitude -0.14, which means that the sensor measures the water level $14\ [cm]$ less then it actually is. Then the sensor fault increases every 20

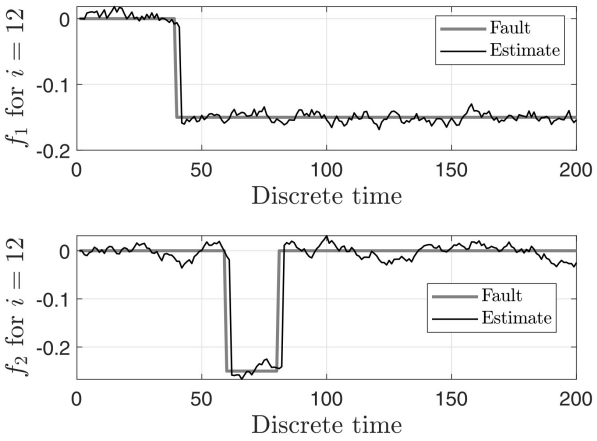


Fig. 9. Sensor faults and their estimates in a faulty trial, $i = 12$ for the fault scenario F-Sc-1.

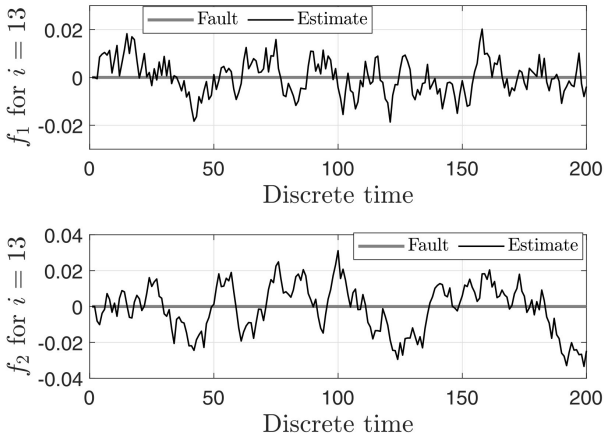


Fig. 10. Sensor faults and their estimates in a fault-free trial, $i = 13$.

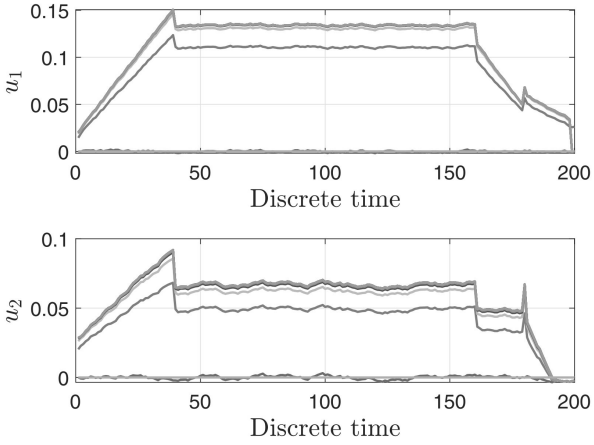


Fig. 11. Control inputs for both pumps along all the trails.

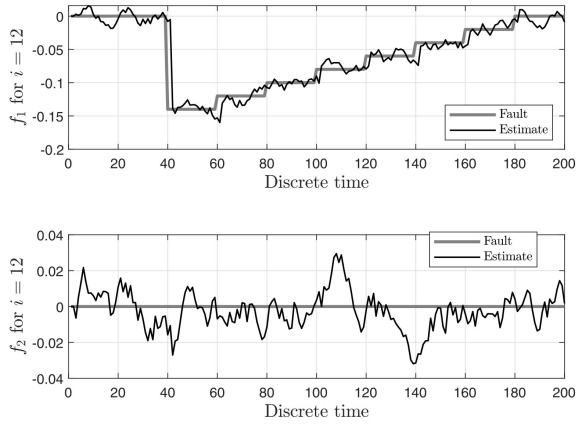


Fig. 12. Real sensor faults with their estimates provided with the fault scenario F-Sc-2.

discrete-time steps with magnitude 0.02 and stops with value 0 at $k = 180$. The results obtained with this scenario are presented in Fig. 12. In such a case, the fault estimate identify the real fault with a quite well accuracy which confirm the efficiency of the proposed approach.

6. Concluding remarks

This paper presents a solution to the problem of control design for a system modeled using a fuzzy Takagi–Sugeno framework. The main issue addressed was the impact of potential sensor faults on the designed control scheme. Additionally, it was assumed that the considered system is influenced by disturbances and noises. Several goals were set when designing the control scheme. The first goal was to achieve a prescribed reference signal at the system output, which was accomplished by implementing Iterative Learning Control. This was achieved by defining an additional signal, the so-called tracking error, i.e., the difference between the reference and the current system output. In the next step, the ILC scheme was introduced in the form of a Discrete Linear Repeatable Process, where the output of this model was the tracking error. For the obtained DLRP, the research results related to the so-called stability along the trial in a closed feedback loop were applied. Importantly, stability along the trial ensures the convergence of the tracking error to zero (therefore, the output of the original considered system aligns with a predefined reference signal). The second objective of the designed control scheme was the ability to respond to potential sensors faults. Due to the fact that the actual faults signals are not available to be measured, the fault estimator was designed and implemented. Additionally, it was assumed that the operating system may be disturbed and noised. In order to minimize this influence on both the estimator and the resulting ILC control scheme, the $\mathcal{H}_\infty$ methodology was used. The effectiveness of the obtained results was tested and verified in practice

during the process of controlling a two-tank system with predefined fault scenarios. As a future work, the problem of simultaneous actuator/process and sensor faults acting on the considered system can be pointed out.

Acknowledgment

This work was supported in part by the National Science Centre in Poland under the grant no. 2020/37/B/ST7/03280.

References

Abonyi, J. and Babuska, R. (2000). Local and global identification and interpretation of parameters in Takagi–Sugeno fuzzy models, *9th IEEE International Conference on Fuzzy Systems, San Antonio, USA*, pp. 835–840.

Alexiev, K. and Georgieva, O. (2004). Improved fuzzy clustering for identification of Takagi–Sugeno model, *Intelligent Systems—2nd International IEEE Conference, Varna, Bulgaria*, pp. 213–218.

Arimoto, S., Kawamura, S. and Miyazaki, F. (1984). Bettering operation of robots by learning, *Journal of Robotic Systems* **1**(2): 123–140.

Bolder, J., Kleinendorst, S. and Oomen, T. (2018). Data-driven multivariable ILC: Enhanced performance by eliminating L and Q filters, *International Journal of Robust and Nonlinear Control* **28**(12, SI): 3728–3751.

Bristow, D.A., Tharayil, M. and Alleyne, A.G. (2006). A survey of iterative learning control, *IEEE Control Systems Magazine* **26**(3): 96–114.

de Oliveira, M.C., Bernussou, J. and Geromel, J.C. (1999). A new discrete-time robust stability condition, *Systems & Control Letters* **37**(4): 261–265.

Deng, S. and Yang, L. (2016). Reliable control design of discrete-time Takagi–Sugeno fuzzy systems with actuator faults, *Neurocomputing* **173**(3): 1784– 1788.

Dong, J. (2023). Robust data-driven iterative learning control for linear-time-invariant and Hammerstein–Wiener systems, *IEEE Transactions on Cybernetics* **53**(2): 1144–1157.

Doyle, J., Glover, K., Khargonekar, P. and Francis, B. (1989). State-space solutions to standard H_2 and H_∞ control-problems, *IEEE Transactions on Automatic Control* **34**(8): 831–847.

Gao, Z.-F., Lin, J.-X. and Cao, T. (2015). Robust fault tolerant tracking control design for a linearized hypersonic vehicle with sensor fault, *International Journal of Control, Automation and Systems* **13**(3): 672–679.

Hedrea, E.-L., Precup, R.-E., Bojan-Dragos, C.-A., Hedrea, C., Ples, D. and Popovici, D. (2019). Cascade control solutions for level control of vertical three tank systems, *IEEE 13th International Symposium on Applied Computational Intelligence and Informatics (SACI), Timisoara, Romania*, pp. 352–357.

Janssens, P., Pipeleers, G. and Swevers, J. (2013). A data-driven constrained norm-optimal iterative learning control framework for LTI systems, *IEEE Transactions on Control Systems Technology* **21**(2): 546–551.

Kukurowski, N., Mrugalski, M., Pazera, M. and Witczak, M. (2022). Fault-tolerant tracking control for a non-linear twin-rotor system under ellipsoidal bounding, *International Journal of Applied Mathematics and Computer Science* **32**(2): 171–183, DOI: 10.34768/amcs-2022-0013.

Leal-Leal, I.E. and Alcorta-Garcia, E. (2023). An efficient fault tolerant control scheme for Euler–Lagrange systems, *International Journal of Applied Mathematics and Computer Science* **33**(2): 219–228, DOI: 10.34768/amcs-2023-0017.

Li, H. and Fu, M. (1997). A linear matrix inequality approach to robust h_∞ filtering, *IEEE Trans. Signal Processing* **45**(9): 2338–2350.

Li, X., Xu, J.-X. and Huang, D. (2014). An iterative learning control approach for linear systems with randomly varying trial lengths, *IEEE Transactions on Automatic Control* **59**(7): 1954–1960.

Liu, G. and Hou, Z. (2024). Adaptive iterative learning fault-tolerant control for state constrained nonlinear systems with randomly varying iteration lengths, *IEEE Transactions on Neural Networks and Learning Systems* **35**(2): 1735–1749.

Liu, X., Ma, L., Kong, X. and Lee, K.Y. (2022). An efficient iterative learning predictive functional control for nonlinear batch processes, *IEEE Transactions on Cybernetics* **52**(6): 4147–4160.

Pazera, M., Sulikowski, B., Kukurowski, N., Witczak, M. and Aubrun, C. (2021). A fault-tolerant iterative learning control for Takagi–Sugeno fuzzy systems, *5th Conference on Control and Fault Tolerant Systems, SysTol 2021, St. Rafael, France*, pp. 267–272.

Pan, S.J. and Yang, Q. (2010). A survey on transfer learning, *IEEE Transactions on Knowledge and Data Engineering* **22**(10): 1345–1359.

Paszke, W., Rogers, E., Gałkowski, K. and Cai, Z. (2013). Robust finite frequency range iterative learning control design and experimental verification, *Control Engineering Practice* **21**(10): 1310–1320.

Rogers, E., Chu, B., Freeman, C.T. and Lewin, P.L. (2023). *Iterative Learning Control Algorithms and Experimental Benchmarking*, Wiley, Hoboken.

Rogers, E., Gałkowski, K. and Owens, D.H. (2007). *Control Systems Theory and Applications for Linear Repetitive Processes*, Springer, Berlin/Heidelberg.

Saif, M. and Guan, Y. (1993). A new approach to robust fault-detection and identification, *IEEE Transactions On Aerospace And Electronic Systems* **29**(3): 685–695.

Shen, D. (2018). Iterative learning control with incomplete information: A survey, *IEEE-CAA Journal of Automatica Sinica* **5**(5): 885–901.

Sornmo, O., Bernhardsson, B., Kroling, O., Gunnarsson, P. and Tenghamn, H. (2016). Frequency-domain iterative learning control of a marine vibrator, *Control Engineering Practice* **47**: 70–80.

Sulikowski, B., Galkowski, K., Rogers, E. and Kummert, A. (2020). Robust iterative learning control for ladder circuits with mixed uncertainties, *16th International Conference on Control, Automation, Robotics and Vision, ICARCV 2020, Shenzhen, China*, pp. 932–937.

Tao, H., Zheng, J., Wei, J., Paszke, W., Rogers, E. and Stojanovic, V. (2023). Repetitive process based indirect-type iterative learning control for batch processes with model uncertainty and input delay, *Journal of Process Control* **132**: 1–12.

Takagi, T. and Sugeno, M. (1985). Fuzzy identification of systems and its application to modeling and control, *IEEE Transactions on Systems, Man and Cybernetics* **15**(1): 116–132.

Wang, J.-S. and Yang, G.-H. (2016). Data-driven output-feedback fault-tolerant compensation control for digital PID control systems with unknown dynamics, *IEEE Transactions on Industrial Electronics* **63**(11): 7029–7039.

Wang, L., Li, B., Yu, J., Zhang, R. and Gao, F. (2018). Design of fuzzy iterative learning fault-tolerant control for batch processes with time-varying delays, *Optimal Control Applications and Methods* **39**(6): 1887–1903.

Wang, Y. and Wang, Z. (2022). Data-driven model-free adaptive fault-tolerant control for a class of discrete-time systems, *IEEE Transactions on Circuits and Systems II: Express Briefs* **69**(1): 154–158.

Witczak, M. (2007). *Modelling and Estimation Strategies for Fault Diagnosis of Non-Linear Systems. From Analytical to Soft Computing Approaches*, Springer, Berlin.

Witczak, M., Pazera, M., Majdzik, P. and Matysiak, R. (2024). Development of a guaranteed minimum detectable sensor fault diagnosis scheme, *International Journal of Applied Mathematics and Computer Science* **34**(3): 409–423, DOI:10.61822/amcs-2024-0029.

Xu, T., Yu, H., Yu, J. and Meng, X. (2020). Adaptive disturbance attenuation control of two tank liquid level system with uncertain parameters based on port-controlled Hamiltonian, *IEEE Access* **8**: 47384–47392.

Yu, X., Hou, Z., Polycarpou, M.M. and Duan, L. (2021). Data-driven iterative learning control for nonlinear discrete-time MIMO systems, *IEEE Transactions on Neural Networks and Learning Systems* **32**(3): 1136–1148.

Zemouche, A., Boutayeb, M. and Bara, G.I. (2008). Observers for a class of Lipschitz systems with extension to H_∞ performance analysis, *Systems & Control Letters* **57**(1): 18–27.

Zhang, J., Qian, K., Luo, H., Liu, Y., Qiao, X., Xu, X. and Tian, J. (2025). Process monitoring for tower pumping units under variable operational conditions: From an integrated multitasking perspective, *Control Engineering Practice* **156**: 106229.



Marcin Pazera was born in Poland in 1990. He received his MSc degree in control engineering and robotics and his PhD degree in automatic control, electronics and electrical engineering in 2015 and 2022, respectively, both from the University of Zielona Góra, Poland. Currently, he is an assistant professor at the Institute of Control and Computation Engineering there. Marcin Pazera has published altogether 52 papers in international journals, book chapters and conference proceedings. His present research interests include fault detection and isolation (FDI), fault-tolerant control (FTC) as well as iterative learning control (ILC) and embedded systems. ORCID: 0000-0003-2469-7570.



Bartłomiej Sulikowski received his DSc and PhD, degrees from the University of Zielona Góra, Poland, in 2019 and 2006, respectively. His research interests cover multidimensional (nD) systems, linear repetitive processes, classes of spatially interconnected systems modeled as 2D/nD systems, iterative learning control (ILC) and applications of numerical methods to control problems for nD systems. Recently, he has turned his interest towards fault-tolerant control methods for 2D/nD systems. For many years he has been a member of teams carrying out the national grants funded by the National Centre of Science, Poland, and international ones (e.g., Polonium, DAAD). His publication record includes over 40 papers in the world-known journals and conference proceedings. ORCID: 0000-0001-9860-8230.



Marcin Witczak was born in Poland in 1973, received his MSc degree in electrical engineering from the University of Zielona Góra, Poland, his PhD degree in automatic control and robotics from the Wrocław University of Technology, Poland, and the his DSc degree in electrical engineering from the University of Zielona Góra, in 1998, 2002 and 2007, respectively. In 2015 he was granted a full professorial title. Since then, Marcin Witczak has been a professor of automatic control and robotics at the Institute of Control and Computation Engineering, University of Zielona Góra. His current research interests include computational intelligence, fault detection and isolation (FDI), fault-tolerant control (FTC), as well as experimental design and control theory. Marcin Witczak has published more than 200 papers in international journals and conference proceedings. He is an author of four monographs and 30 book chapters. Since 2015, he has been a member of the Committee on Automatic Control and Robotics Committee of the Polish Academy of Sciences. As of 2018, he is also an associated editor of *ISA Transactions*. ORCID: 0000-0002-0031-0004.

Received: 13 November 2024
Revised: 2 April 2025
Re-revised: 12 & 23 May 2025
Accepted: 1 July 2025